8020 *Inorg. Chem.* **2009**, *48*, 8020–8029
DOI: 10.1021/ic900689k

Inorganic Chemistry
Article

Ligand Exchange Reactions and Hydroamination with Tris(oxazolinyl)borato Yttrium Compounds

Andrew V. Pawlikowski, Arkady Ellern, and Aaron D. Sadow*

Department of Chemistry, Iowa State University, Ames, Iowa 50011

Received April 9, 2009

Ligand substitution reactions and catalytic hydroamination/cyclization of aminoalkenes have been studied with a new oxazolinylborato yttrium compound, tris(4,4-dimethyl-2-oxazolinyl)phenylborato bis(trimethylsilylmethyl)yttrium ([Y(κ^3-To^M)(CH$_2$SiMe$_3$)$_2$(THF)], **1**). THF exchange in **1** is rapid at room temperature, and activation parameters obtained by simulation of ^{1}H NMR spectra acquired from 190 to 280 K are consistent with a dissociative mechanism ($\Delta S^‡ = 30 \pm 1$ e.u., $\Delta G^‡ = 11.9$ kcal mol^{-1} at 243 K). The related phosphine oxide adduct [Y(κ^3-To^M)(CH$_2$SiMe$_3$)$_2$(OPPh$_3$)] (**2**) also undergoes exchange via OPPh$_3$ dissociation with a much higher barrier ($\Delta G^‡ = 15.0$ kcal mol^{-1} at 320 K). Compound **1** reacts with the amines ^{t}BuNH$_2$, *para*-MeC$_6$H$_4$NH$_2$, and 2,6-^{i}Pr$_2$C$_6$H$_3$NH$_2$ to provide six-coordinate [Y(κ^3-To^M)(NHR)$_2$(THF)] (**3**: R = ^{t}Bu; **4**: R = *para*-MeC$_6$H$_4$) and five-coordinate [Y(κ^3-To^M)(NH-2,6-^{i}Pr$_2$C$_6$H$_3$)$_2$] (**6**). These oxazolinylborato yttrium compounds are precatalysts for the cyclization of aminoalkenes; the kinetics of catalytic conversion indicate zero-order substrate dependence and first-order catalyst dependence. Kinetic investigations of ligand exchange processes and hydroamination reactions indicate that the tris(oxazolinyl)borato-yttrium interaction is robust even in the presence of excess phosphine oxide and primary and secondary amines.

Introduction

Exchange of coordinated product for substrate is an important part of catalytic chemistry, and thus rare earth organometallic compounds are valuable in catalysis because of their facile ligand substitutions.[1] However, undesired substitution of ancillary ligands can diminish yields, lower selectivity, and provide pathways for decomposition. Additionally, exchange reactions can be difficult to detect if the thermodynamically favored product contains kinetically labile ancillary ligands. A key challenge in organo-rare earth element chemistry is the discovery of new robust spectator ligands that control the selectivity of reactions, such as ligand exchange, at the remaining bonding sites. In this context, tridentate, *fac*-coordinating monoanionic ligands are expected to be useful for trivalent rare earth chemistry because their charge and the chelate effect inhibit ancillary ligand dissociation, whereas two reactive valences remain available for bonding to additional anionic ligands.

C_{3v}-symmetric ligands, such as the anionic borate-containing tris(pyrazolyl)borates (Tp),[2] tris(phosphino)borates,[3] tris(carbene)borates,[4] and tris(sulfido)borates,[5] have allowed for the stabilization of reactive moieties bonded to metal centers. Recently, the related zwitterionic C_2-symmetric bis(oxazolinyl)borate (borabox)[6] and neutral tris-oxazoline ligands (tris-ox)[7] have provided optically active scorpionate-like ligands. We have recently contributed to this area with tris(oxazolinyl)borates[8] that combine zwitterionic and tridentate features, providing ligands reasonably described as sterically and electronically modified tris(pyrazolyl)borates. The zwitterionic nature, tridentate binding motif, and steric protection afforded by tris(oxazolinyl)borates suggest that they would be good ancillary ligands for rare earth centers. Thus, we began to synthesize new compounds containing the tris(4,4-dimethyl-2-oxazolinyl)borate ligand

*Corresponding author. E-mail: sadow@iastate.edu.

(1) (a) Watson, P. L.; Parshall, G. W. *Acc. Chem. Res.* **1985**, *18*, 51–56. (b) Anwander, R. *Top. Organomet. Chem.* **1999**, *2*, 1–61. (c) Sastri, V. S.; Bünzli, J.-C.; Rao, V. R.; Rayudu, G. V. S.; Perumareddi, J. R. *Modern Aspects of Rare Earths and Their Complexes*; Elsevier: Amsterdam, 2003.

(2) Trofimenko, S. *Scorpionates: The Coordination Chemistry of Polypyrazolylborate Ligands*; Imperial College Press: London, 1999.

(3) (a) Peters, J. C.; Feldman, J. D.; Tilley, T. D. *J. Am. Chem. Soc.* **1999**, *121*, 9871–9872. (b) Betley, T. A.; Peters, J. C. *J. Am. Chem. Soc.* **2003**, *125*, 10782–10783.

(4) (a) Fränkel, R.; Kernbach, U.; Bakola-Christianopoulou, M.; Plaia, U.; Suter, M.; Ponikwar, W.; Nöth, H.; Moinet, C.; Fehlhammer, W. P. *J. Organomet. Chem.* **2001**, *617*−*618*, 530–545. (b) Nieto, I.; Cervantes-Lee, F.; Smith, J. M. *Chem. Commun.* **2005**, 3811–3813. (c) Cowley, R. E.; Bontchev, R. P.; Duesler, E. N.; Smith, J. M. *Inorg. Chem.* **2006**, *45*, 9771–9779.

(5) Ge, P.; Haggerty, B. S.; Rheingold, A. L.; Riordan, C. G. *J. Am. Chem. Soc.* **1994**, *116*, 8406–8407.

(6) Mazet, C.; Köhler, V.; Pfaltz, A. *Angew. Chem., Int. Ed.* **2005**, *44*, 4888–4891.

(7) (a) Bellemin-Laponnaz, S.; Gade, L. H. *Angew. Chem., Int. Ed.* **2002**, *41*, 3473–3475. (b) Gade, L. H.; Bellemin-Laponnaz, S. *Chem.—Eur. J.* **2008**, *14*, 4142–4152.

(8) (a) Dunne, J. F.; Su, J. C.; Ellern, A.; Sadow, A. D. *Organometallics* **2008**, *27*, 2399–2401. (b) Baird, B.; Pawlikowski, A. V.; Su, J.; Wiench, J. W.; Pruski, M.; Sadow, A. D. *Inorg. Chem.* **2008**, *47*, 10208–10210.

Published on Web 07/08/2009

(abbreviated To^M) and investigate their chemistry in substitution reactions and catalysis.

Tris(pyrazolyl)borate rare earth compounds are well-known,[9] but the mechanisms of neutral ligand substitutions in mono-tris(pyrazolyl)borate complexes still require investigation. For example, evidence favors an associative mechanism for substitution of THF in $[Y(\kappa^3\text{-Tp*})Cl_2(THF)]$ (Tp* = tris(3,5-dimethyl-1-pyrazolyl)borohydride) even though the yttrium(III) center is six-coordinate.[10] In contrast, the bulky $[Y(\kappa^3\text{-Tp}^{tBuMe})(CH_2SiMe_3)_2]$ is five-coordinate.[11] Establishing mechanism(s) for ligand exchange pathways in To^MLnR_2L compounds (eq 1, Ln = group 3 or lanthanide element) is clearly important for understanding substrate coordination to active sites in catalytic processes.

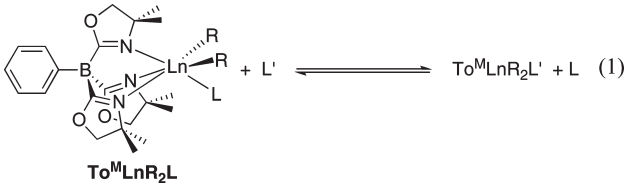

(1)

Additionally, substitutions of alkyl groups via protonolytic ligand elimination reactions have not been well investigated in the $TpLnR_2(L)$-type systems,[10−12] although these reactions are well-known with other ancillary ligands in rare earth element chemistry and are steps in the proposed mechanism for rare earth element catalyzed hydroamination/cyclization of aminoalkenes.[13] Thus, we were interested to investigate alkyl-group protonolysis reactions with $[Y(\kappa^3\text{-To}^M)(CH_2SiMe_3)_2(THF)]$ (**1**) to establish the To^M-Y interaction as inert to cleavage in the presence of excess amine (eq 2).

$$To^MLnR_2L + 2\ H\text{-}NR'_2 \rightarrow To^MLn(NR'_2)_2L + 2\ H\text{-}R \quad (2)$$

Additional motivation was that few bis(amido) compounds of the type $TpLn(NR_2)_2$ have been described,[14] although rare earth amido compounds have wide-ranging chemistry. The reported catalytic chemistry of mono-tris(pyrazolyl)borate and tris-ox rare earth compounds has primarily focused on olefin polymerization,[10,15] and our tris(oxazolinyl)borate compounds might provide new catalytic chemistry for scorpionate-type complexes. In particular, hydroamination/cyclization of aminoolefins has recently received significant attention as an efficient method for preparing nitrogen-containing heterocycles.[13,16,17] Although most rare earth hydroamination/cyclization catalysts contain dianionic ancillary ligand sets,[18] fewer catalysts contain one monoanionic ancillary ligand and two reactive valences.[19,20] Although oxazoline ligands are common ancillary ligands in transition-metal chemistry, few oxazoline-containing complexes have been studied in rare earth hydroamination catalyses.[20]

Here we describe the synthesis and structural characterization of the first tris(oxazolinyl)borate yttrium alkyl and amide compounds, ligand exchange reactions at the reactive yttrium centers, and their catalytic properties in hydroamination/cyclization of aminoalkenes. We have investigated the kinetics of ligand exchange and hydroamination reactions, and these measurements show that the yttrium-To^M interaction is robust under catalytic conditions, whereas the yttrium alkyl, amido, and neutral ligands react rapidly.

Experimental Section

General Procedures. All reactions were performed under a dry argon atmosphere using standard Schlenk techniques or under a nitrogen atmosphere in a glovebox, unless otherwise indicated. Water and oxygen were removed from benzene, toluene, pentane, diethyl ether, and tetrahydrofuran solvents using an IT PureSolv system. Benzene-d_6, tetrahydrofuran-d_8, and toluene-d_8 were heated to reflux over Na/K alloy and vacuum-transferred. Anhydrous YCl_3 was purchased from Strem and used as received. 2,6-diisopropylaniline and *tert*-butylamine were distilled from CaH_2 prior to use and stored over 4 Å mol. sieves in the glovebox, and *p*-toluidine was purified by sublimation. The aminoalkenes 4-penten-1-amine,[13b] *N*-methyl-2,2-diphenyl-4-penten-1-amine,[21] 2,2-diphenyl-4-penten-1-amine, and 2,2-dimethyl-4-penten-1-amine,[20]

(9) Marques, N.; Sella, A.; Takats, J. *Chem. Rev.* **2002**, *102*, 2137–2159.
(10) (a) Long, D. P.; Bianconi, P. A. *J. Am. Chem. Soc.* **1996**, *118*, 12453–12454. (b) Long, D. P.; Chandrasekaran, A.; Day, R. O.; Bianconi, P. A.; Rheingold, A. L. *Inorg. Chem.* **2000**, *39*, 4476–4487.
(11) (a) Cheng, J.; Saliu, K.; Kiel, G. Y.; Ferguson, M. J.; McDonald, R.; Takats, J. *Angew. Chem., Int. Ed.* **2008**, *47*, 4910–4913. (b) Litlabφ, R.; Zimmermann, M.; Saliu, K.; Takats, J.; Türnroos, K. W.; Anwander, R. *Angew. Chem., Int. Ed.* **2008**, *47*, 9560–9564. (c) Zimmermann, M.; Takats, J.; Kiel, G.; Törnroos, K. W.; Anwander, R. *Chem. Commun.* **2008**, 612–614.
(12) Blackwell, J.; Lehr, C.; Sun, Y.; Piers, W. E.; Pearce-Batchilder, S. D.; Zaworotko, M. J.; Young, V. G., Jr. *Can. J. Chem.* **1997**, *75*, 702–711.
(13) (a) Gagné, M. R.; Marks, T. J. *J. Am. Chem. Soc.* **1989**, *111*, 4108–4109. (b) Gagné, M. R.; Stern, C. L.; Marks, T. J. *J. Am. Chem. Soc.* **1992**, *114*, 275–294.
(14) (a) Roitershtein, D.; Domingos, A.; Pereira, L. C. J.; Ascenso, J. R.; Marques, N. *Inorg. Chem.* **2003**, *42*, 7666–7673. (b) Foley, T. J.; Harrison, B. S.; Knefely, A. S.; Abboud, K. A.; Reynolds, J. R.; Schanze, K. S.; Boncella, J. M. *Inorg. Chem.* **2003**, *42*, 5023–5032.
(15) (a) Ward, B. D.; Bellemin-Laponnaz, S.; Gade, L. H. *Angew. Chem., Int. Ed.* **2005**, *44*, 1668–1671. (b) Lukesova, L.; Ward, B. D.; Bellemin-Laponnaz, S.; Wadepohl, H.; Gade, L. H. *Organometallics* **2007**, *26*, 4652–4657. (c) Lukesova, L.; Ward, B. D.; Bellemin-Laponnaz, S.; Wadepohl, H.; Gade, L. H. *Dalton Trans.* **2007**, 920–922.
(16) (a) Molander, G. A.; Romero, J. A. C. *Chem. Rev.* **2002**, *102*, 2161–2185. (b) Hong, S.; Marks, T. J. *Acc. Chem. Res.* **2004**, *37*, 673–686. (c) Hultzsch, K. C. *Adv. Synth. Catal.* **2005**, *347*, 367–391. (d) Müller, T. E.; Hultzsch, K. C.; Yus, M.; Foubelo, F.; Tada, M. *Chem. Rev.* **2008**, *108*, 3795–3892.
(17) (a) Molander, G. A.; Dowdy, E. D. *J. Org. Chem.* **1999**, *64*, 6515–6517. (b) Ryu, J.-S.; Marks, T. J.; McDonald, F. E. *Org. Lett.* **2001**, *3*, 3091–3094. (c) Hong, S.; Marks, T. J. *J. Am. Chem. Soc.* **2002**, *124*, 7886–7887. (d) Ryu, J.-S.; Marks, T. J.; McDonald, F. E. *J. Org. Chem.* **2004**, *69*, 1038–1052.
(18) (a) Tian, S.; Arredondo, V. M.; Stern, C. L.; Marks, T. J. *Organometallics* **1999**, *18*, 2568–2570. (b) Kim, Y. K.; Livinghouse, T. *Angew. Chem., Int. Ed.* **2002**, *41*, 3645–3647. (c) O'Shaughnessy, P. N.; Knight, P. D.; Morton, C.; Gillespie, K. M.; Scott, P. *Chem. Commun.* **2003**, 1770–1771. (d) Gribkov, D. V.; Hampel, F.; Hultzsch, K. C. *Eur. J. Inorg. Chem.* **2004**, 4091–4101. (e) Kim, J. Y.; Livinghouse, T. *Org. Lett.* **2005**, *7*, 1737–1739. (f) Collin, J.; Daran, J.-C.; Jacquet, O.; Schulz, E.; Trifonov, A. *Chem.—Eur. J.* **2005**, *11*, 3455–3462. (g) Meyer, N.; Zulys, A.; Roesky, P. W. *Organometallics* **2006**, *25*, 4179–4182. (h) Gribkov, D. V.; Hultzsch, K. C.; Hampel, F. *J. Am. Chem. Soc.* **2006**, *128*, 3748–3759. (i) Yu, X.; Marks, T. J. *Organometallics* **2007**, *26*, 365–376.
(19) (a) Zulys, A.; Panda, T. K.; Gamer, M. T.; Roesky, P. W. *Chem. Commun.* **2004**, 2584–2585. (b) Lauterwasser, F.; Hayes, P. G.; Bräse, S.; Piers, W. E.; Schafer, L. L. *Organometallics* **2004**, *23*, 2234–2237. (c) Bambirra, S.; Tsurugi, H.; Leusen, D.; Hessen, B. *Dalton Trans.* **2006**, 1157–1161.
(20) Hong, S.; Tian, S.; Metz, M. V.; Marks, T. J. *J. Am. Chem. Soc.* **2003**, *125*, 14768–14783.
(21) Stubbert, B. D.; Marks, T. J. *J. Am. Chem. Soc.* **2007**, *129*, 4253–4271.

Li[To^M],[8a] and [Y(CH$_2$SiMe$_3$)$_3$(THF)$_2$][22] were prepared by published procedures. Anhydrous H[To^M] was prepared from Li[To^M] and triethylammonium chloride in CH_2Cl_2. ^{1}H, ^{11}B, ^{13}C{^{1}H}, and ^{29}Si{^{1}H} spectra were collected on Bruker DRX-400, DRX-500, and AV-600 spectrometers. ^{15}N chemical shifts were determined by ^{1}H−^{15}N HMBC experiments on a Bruker Avance II 700 spectrometer with a Bruker Z-gradient inverse TXI ^{1}H/^{13}C/^{15}N 5 mm cryoprobe; ^{15}N chemical shifts were originally referenced to liquid NH_3 and recalculated to the CH_3NO_2 chemical shift scale by adding −381.9 ppm. ^{11}B NMR spectra were referenced to an external sample of $BF_3 \cdot Et_2O$. Elemental analyses were performed using a Perkin-Elmer 2400 Series II CHN/S by the Iowa State Chemical Instrumentation Facility. X-ray diffraction data was collected on a Bruker-AXS SMART 1000 CCD diffractometer using Bruker-AXS SHELXTL software.

[Y(κ^3-To^M)(CH$_2$SiMe$_3$)$_2$(THF)] (1). A THF solution of H[To^M] (0.761 g, 1.99 mmol) was added in a dropwise fashion to a pentane solution of [Y(CH$_2$SiMe$_3$)$_3$(THF)$_2$] (0.988 g, 2.0 mmol) at room temperature. Pale yellow crystals of **1** formed after standing at −30 °C for 2 days. The crystals were isolated by filtration, washed with pentane, and dried under vacuum to give 1.09 g of **1** (1.52 mmol, 77%). X-ray quality crystals of **1** were grown from a concentrated toluene solution of [Y(κ^3-To^M)(CH$_2$SiMe$_3$)$_2$(THF)] layered with hexane at −30 °C. ^{1}H NMR (400 MHz, benzene-d_6): δ −0.34 (d, $^2J_{YH}$ = 2.8 Hz, 4 H, YC*H*$_2$SiMe$_3$), 0.45 (s, 18 H, CH$_2$Si*Me*$_3$), 1.20 (s, 18 H, CNC*Me*$_2$CH$_2$O), 1.35 (m, 4 H, THF β-C*H*$_2$), 3.33 (s, 6 H, CNCMe$_2$C*H*$_2$O), 3.89 (m, 4 H, THF α-C*H*$_2$), 7.35 (t, $^3J_{HH}$ = 7.2 Hz, 1 H, *para*-C$_6$H$_5$), 7.53 (t, $^3J_{HH}$ = 7.2 Hz, 2 H, *meta*-C$_6$H$_5$), 8.23 (d, $^3J_{HH}$ = 7.2 Hz, 2 H, *ortho*-C$_6$H$_5$). ^{13}C{^{1}H} NMR (100 MHz, benzene-d_6): δ 5.55 (CH$_2$Si*Me*$_3$), 25.29 (THF β-*C*H$_2$), 28.28 (CNC*Me*$_2$CH$_2$O), 37.08 (d, $^1J_{YC}$ = 35 Hz, Y*C*H$_2$SiMe$_3$), 67.92 (CN*C*Me$_2$CH$_2$O), 71.09 (THF α-*C*H$_2$), 79.56 (CNCMe$_2$*C*H$_2$O), 125.90 (*para*-C$_6$H$_5$), 126.93 (*meta*-C$_6$H$_5$), 136.64 (*ortho*-C$_6$H$_5$). ^{11}B NMR (128 MHz, benzene-d_6): δ −18.2. ^{15}N{^{1}H} NMR (71 MHz, benzene-d_6): δ −141.7. ^{29}Si{^{1}H} NMR (79.5 MHz, benzene-d_6): δ −2.7 ($^2J_{YSi}$ = 4.6 Hz). IR (KBr, cm^{-1}): 2961 (m), 2892 (m), 1568 (s), 1463 (w), 1368 (w), 1272 (m), 1248 (m), 1234 (w), 1194 (m), 1149 (m), 1024 (w), 994 (m), 922 (w), 860 (s), 810 (w). Anal. Calcd for $C_{33}H_{59}BN_3O_4Si_2Y$: C, 55.22; H, 8.29; N, 5.85. Found: C, 54.98; H, 8.12; N, 5.83. mp 185 °C (dec.)

[Y(κ^3-To^M)(CH$_2$SiMe$_3$)$_2$(OPPh$_3$)] (2). Compound **1** (0.116 g, 0.162 mmol) was dissolved in benzene (3 mL) and triphenylphosphine oxide (0.045 g, 0.162 mmol) was added. After 10 min, the volatiles were removed and the remaining solid was washed with pentane and dried under vacuum to yield 0.108 g of analytically pure [Y(κ^3-To^M)(CH$_2$SiMe$_3$)$_2$(OPPh$_3$)] (**2**) as an off-white solid (0.117 mmol, 73%). ^{1}H NMR (400 MHz, benzene-d_6): δ −0.21 (d, $^2J_{YH}$ = 2.4 Hz, 4 H, YC*H*$_2$SiMe$_3$), 0.48 (s, 18 H, CH$_2$Si*Me*$_3$), 0.88 (br s, 6 H, CNC*Me*$_2$CH$_2$O), 1.14 (br s, 6 H, CNC*Me*$_2$CH$_2$O), 1.56 (br s, 6 H, CNC*Me*$_2$CH$_2$O), 3.17 (br s, 2H, CNCMe$_2$C*H*$_2$O), 3.42 (br m, 4 H, CNCMe$_2$C*H*$_2$O), 7.04 (m, 9 H, OP*Ph*$_3$), 7.37 (t, $^3J_{HH}$ = 7.2 Hz, 1 H, *para*-C$_6$H$_5$), 7.58 (t, $^3J_{HH}$ = 7.6 Hz, 2 H, *meta*-C$_6$H$_5$), 7.65 (m, 6 H, OP*Ph*$_3$), 8.49 (d, $^3J_{HH}$ = 7.2 Hz, 2 H, *ortho*-C$_6$H$_5$). ^{13}C{^{1}H} NMR (125 MHz, benzene-d_6): δ 5.74 (CH$_2$Si*Me*$_3$), 27.05 (br, CNC*Me*$_2$CH$_2$O), 29.30 (br, CNC*Me*$_2$CH$_2$O), 35.07 (d, $^1J_{YC}$ = 35 Hz, Y*C*H$_2$SiMe$_3$), 67.96 (br, CN*C*Me$_2$CH$_2$O), 68.45 (br, CNCMe$_2$CH$_2$O), 78.62 (br, CNCMe$_2$*C*H$_2$O), 79.89 (br, CNCMe$_2$*C*H$_2$O), 125.63 (*para*-C$_6$H$_5$), 126.82 (*meta*-C$_6$H$_5$), 129.24 (d, $^1J_{PC}$ = 108 Hz, OP*Ph*$_3$), 129.36 (d, $^4J_{PC}$ = 12.8 Hz, OP*Ph*$_3$), 133.58 (d, $^3J_{PC}$ = 10.8 Hz, OP*Ph*$_3$), 133.93 (d, $^5J_{PC}$ = 2.3 Hz, OP*Ph*$_3$), 136.90 (*ortho*-C$_6$H$_5$). ^{11}B NMR (128 MHz, benzene-d_6): δ −18.3. ^{29}Si{^{1}H} NMR (79.5 MHz, benzene-d_6): δ −3.9 (d, $^2J_{YSi}$ = 4.3 Hz). ^{31}P{^{1}H} NMR (162 MHz, benzene-d_6): δ 36.69 (d, $^2J_{YP}$ = 9.8 Hz). IR (KBr, cm^{-1}): 3055 (w), 2959 (s), 2883 (m), 1575 (s), 1462 (w), 1438 (s), 1367 (w), 1270 (m), 1248 (m), 1195 (m), 1152 (s), 1120 (s), 1091 (w), 997 (m), 973 (w), 862 (s), 809 (w). Anal. Calcd for $C_{47}H_{66}BN_3O_4PSi_2Y$: C, 61.10; H, 7.20; N, 4.55. Found: C, 61.19; H, 7.35; N, 4.62. mp 205 °C (dec.)

[Y(κ^3-To^M)(NH^{t}Bu)$_2$(THF)] (3). *Tert*-butylamine (14.9 μL, 0.142 mmol) was added to a solution of **1** (0.051 g, 0.071 mmol) in benzene at ambient temperature. After 5 min, the volatiles were removed from the reaction mixture, and the resulting residue was washed with pentane and dried under vacuum to yield 0.035 g of [Y(κ^3-To^M)(NH^{t}Bu)$_2$(THF)] (**3**) as a white powder (0.051 mmol, 73%). ^{1}H NMR (400 MHz, benzene-d_6): δ 1.28 (s, 18 H, CNC*Me*$_2$CH$_2$O), 1.38 (m, 4 H, THF β-C*H*$_2$), 1.56 (s, 18 H, NHC*Me*$_3$), 1.82 (d, $^2J_{YH}$ = 2.0 Hz, 2 H, N*H*CMe$_3$), 3.39, (s, 6 H, CNCMe$_2$C*H*$_2$O), 3.71 (m, 4 H, THF α-C*H*$_2$), 7.36 (t, $^3J_{HH}$ = 7.6 Hz, 1 H, *para*-C$_6$H$_5$), 7.55 (t, $^3J_{HH}$ = 7.6 Hz, 2 H, *meta*-C$_6$H$_5$), 8.36 (d, $^3J_{HH}$ = 7.2 Hz, 2 H, *ortho*-C$_6$H$_5$). ^{13}C{^{1}H} NMR (100 MHz, benzene-d_6): δ 25.74 (THF β-*C*H$_2$), 28.25 (CNC*Me*$_2$CH$_2$O), 37.37 (NHC*Me*$_3$), 53.92 (d, $^2J_{YC}$ = 4.5 Hz, NH*C*Me$_3$), 67.78 (CN*C*Me$_2$CH$_2$O), 69.70 (THF α-*C*H$_2$), 79.18 (CNCMe$_2$*C*H$_2$O), 125.61 (*para*-C$_6$H$_5$), 126.82 (*meta*-C$_6$H$_5$), 136.78 (*ortho*-C$_6$H$_5$). ^{11}B NMR (128 MHz, benzene-d_6): δ −18.3. ^{15}N{^{1}H} NMR (71 MHz, benzene-d_6): δ −141.2 (C*N*CMe$_2$CH$_2$O), −224.6 (*N*HCMe$_3$). IR (KBr, cm^{-1}): 3044 (w), 2961 (s), 2887 (m), 1576 (s), 1462 (w), 1431 (w), 1366 (m), 1347 (w), 1270 (m), 1247 (w), 1195 (m), 1173 (m), 1146 (m), 1028 (w), 972 (s), 920 (w), 887 (w), 836 (w), 788 (w). Anal. Calcd for $C_{33}H_{57}BN_5O_4Y$: C, 57.65; H, 8.36; N, 10.19. Found: C, 57.23; H, 8.27; N, 9.64. mp 195 °C (dec.)

[Y(κ^3-To^M)(NH-*para*-MeC$_6$H$_4$)$_2$(THF)] (4). *para*-Toluidine (0.018 g, 0.167 mmol) and **1** (0.060 g, 0.084 mmol) were dissolved in toluene (2 mL) at ambient temperature. After 5 min, the volatiles were removed from the reaction mixture, and the resulting white powder was washed with pentane and dried under vacuum to afford 0.055 g of analytically pure [Y(κ^3-To^M)(NH-*para*-MeC$_6$H$_4$)$_2$(THF)] (0.073 mmol, 87%). ^{1}H NMR (400 MHz, benzene-d_6): δ 1.12 (br s, 18 H, CNC*Me*$_2$CH$_2$O), 1.34 (m, 4 H, THF β-C*H*$_2$), 2.31 (s, 6 H, NH-*para*-*Me*C$_6$H$_4$), 3.38 (s, 6 H, CNCMe$_2$C*H*$_2$O), 3.77 (m, 4 H, THF α-CH$_2$), 4.66 (s, 2 H, N*H*-*para*-MeC$_6$H$_4$), 6.86 (d, $^3J_{HH}$ = 8.2 Hz, 4 H, NH-*para*-MeC$_6$*H*$_4$), 7.10 (d, $^3J_{HH}$ = 8.2 Hz, 4 H, NH-*para*-MeC$_6$*H*$_4$), 7.37 (t, $^3J_{HH}$ = 7.6 Hz, 1 H, *para*-C$_6$H$_5$), 7.57 (t, $^3J_{HH}$ = 7.6 Hz, 2 H, *meta*-C$_6$H$_5$), 8.30 (d, $^3J_{HH}$ = 7.6 Hz, 2 H, *ortho*-C$_6$H$_5$). ^{13}C{^{1}H} NMR (100 MHz, benzene-d_6): 21.17 (NH-*para*-*Me*C$_6$H$_4$), 25.85 (THF β-*C*H$_2$), 28.18 (CNC*Me*$_2$CH$_2$O), 67.85 (CN*C*Me$_2$CH$_2$O), 70.32 (THF α-*C*H$_2$), 79.77 (CNCMe$_2$*C*H$_2$O), 117.44 (NH-*para*-Me*C*$_6$H$_4$), 122.40 (NH-*para*-Me*C*$_6$H$_4$), 125.98 (*para*-C$_6$H$_5$), 127.03 (*meta*-C$_6$H$_5$), 130.54 (NH-*para*-Me*C*$_6$H$_4$), 136.62 (*para*-C$_6$H$_5$), 155.78 (NH-*para*-Me*C*$_6$H$_4$). ^{11}B NMR (128 MHz, benzene-d_6): δ −18.1. ^{15}N{^{1}H} NMR (71 MHz, benzene-d_6): δ −142.9 (C*N*CMe$_2$CH$_2$O), −231.2 (*N*H-*para*-MeC$_6$H$_4$). IR (KBr, cm^{-1}): 2963 (m), 2929 (m), 2893 (m), 1608 (m), 1570 (s), 1505 (s), 1462 (w), 1431 (w), 1367 (w), 1352 (w), 1297 (m), 1270 (m), 1251 (w), 1192 (m), 1175 (m), 1150 (m), 1103 (w), 1014 (w), 988 (w),

(22) (a) Lappert, M. F.; Pearce, R. *J. Chem. Soc., Chem. Commun.* **1973**, 126. (b) Hultzsch, K. C.; Voth, P.; Beckerle, K.; Spaniol, T. P.; Okuda, J. *Organometallics* **2000**, *19*, 228–243.

973 (w), 922 (w), 854 (w), 816 (m). Anal. Calcd for $C_{39}H_{53}BN_5O_4Y$: C, 61.99; H, 7.07; N, 9.27. Found: C, 62.02; H, 7.02; N, 9.22. mp 132 °C (dec.)

[Y(κ^3-To^M)(NH^{t}Bu)$_2$(NH$_2^t$Bu)] (5). A solution of **1** (0.096 g, 0.134 mmol) in benzene was treated with an excess of *tert*-butylamine (0.3 mL, 2.85 mmol) at room temperature. The volatiles were removed under reduced pressure, and the resulting white powder was redissolved in benzene and treated with another 0.3 mL of *tert*-butylamine. The volatiles were again removed under vacuum to yield 0.085 g of [Y(κ^3-To^M)-(NH^{t}Bu)$_2$(NH$_2^t$Bu)] (**5**) as a white powder (0.123 mmol, 92%). Crystals of **5** suitable for X-ray diffraction were obtained from a concentrated toluene solution layered with pentane at −30 °C. ^{1}H NMR (400 MHz, benzene-d_6): δ 1.26 (s, 18 H, CNCMe_2CH$_2$O), 1.44 (br s, 27 H, NH$_2$CMe_3 and NHCMe_3), 1.97 (br s, 4 H, NH_2CMe$_3$ and NHCMe$_3$), 3.34, (s, 6 H, CNCMe$_2$CH_2O), 7.35 (t, $^3J_{HH}$ = 6.8 Hz, 1 H, *para*-C$_6$H$_5$), 7.54 (t, $^3J_{HH}$ = 7.2 Hz, 2 H, *meta*-C$_6$H$_5$), 8.29 (d, $^3J_{HH}$ = 7.2 Hz, 2 H, *ortho*-C$_6$H$_5$). ^{13}C{^{1}H} NMR (125 MHz, benzene-d_6): δ 28.74 (CNCMe_2CH$_2$O), 35.88 (br, NH$_2$CMe_3 and NHCMe_3), 52.65 (br, NH$_2$$CMe_3$ and NHCMe$_3$), 67.64 (CNCMe$_2$CH$_2$O), 79.20 (CNCMe$_2$CH_2O), 125.68 (*para*-C$_6$H$_5$), 126.86 (*meta*-C$_6$H$_5$), 136.69 (*ortho*-C$_6$H$_5$). ^{11}B NMR (128 MHz, benzene-d_6): δ −18.2. ^{15}N{^{1}H} NMR (71 MHz, benzene-d_6): δ −142.5 (CNCMe$_2$CH$_2$O). IR (KBr, cm^{-1}): 3343 (vw), 3042 (w), 2964 (s), 2875 (m), 1575 (s), 1463 (m), 1431 (w), 1367 (m), 1349 (w), 1270 (m), 1194 (m), 1174 (m), 1147 (m), 1072 (w), 993 (m), 973 (m), 920 (w), 889 (w), 837 (w), 800 (w). Anal. Calcd for $C_{33}H_{60}BN_6O_3Y$: C, 57.56; H, 8.78; N, 12.20. Found: C, 57.91; H, 8.50; N, 12.14. mp 192 °C (dec.)

[Y(κ^3-To^M)(NH-2,6-^{i}Pr$_2$C$_6$H$_3$)$_2$] (6). 2,6-Diisopropylaniline (0.032 mL, 0.169 mmol) was added to a benzene solution of **1** (0.060 g, 0.084 mmol) at ambient temperature, and the reaction mixture was stirred for 5 min. After evaporation of the volatiles, the resulting residue was washed with cold pentane (5 mL) and dried under vacuum, affording [Y(κ^3-To^M)(2,6-^{i}Pr$_2$C$_6$H$_3$NH)$_2$] as a pale yellow powder (0.055 g, 0.067 mmol, 81% yield). ^{1}H NMR (400 MHz, benzene-d_6): δ 1.02 (s, 18 H, CNCMe_2CH$_2$O), 1.37 (d, $^3J_{HH}$ = 6.8 Hz, 24 H, CHMe_2), 3.30 (m, $^3J_{HH}$ = 6.8 Hz, 4 H, CHMe$_2$), 3.35 (s, 6 H, CNCMe$_2$CH_2O), 5.00 (s, 2 H, NH), 6.88 (t, $^3J_{HH}$ = 7.6 Hz, 2 H, NH-2,6-^{i}Pr$_2$C$_6$$H_3$), 7.17 (d, $^3J_{HH}$ = 7.6 Hz, 4 H, NH-2,6-^{i}Pr$_2$C$_6$$H_3$), 7.34 (t, $^3J_{HH}$ = 7.6 Hz, 1 H, *para*-C$_6$H$_5$), 7.52 (t, $^3J_{HH}$ = 7.6 Hz, 2 H, *meta*-C$_6$H$_5$), 8.19 (d, $^3J_{HH}$ = 7.6 Hz, 2 H, *ortho*-C$_6$H$_5$). ^{13}C{^{1}H} NMR (100 MHz, benzene-d_6): δ 24.44 (CHMe_2), 28.01 (CNCMe_2CH$_2$O), 30.25 (*C*HMe$_2$), 67.67 (CNCMe$_2$CH$_2$O), 79.93 (CNCMe$_2$$CH_2$O), 116.54 (NH-2,6-^{i}Pr$_2$C$_6$H$_3$), 123.65 (NH-2,6-^{i}Pr$_2$$C_6H_3$), 126.35 (*para*-C$_6H_5$), 127.33 (*meta*-C$_6H_5$), 133.94 (NH-2,6-^{i}Pr$_2$$C_6H_3$), 136.17 (*ortho*-C$_6H_5$), 152.28 (d, $^2J_{YC}$ = 3.9 Hz, NH-2,6-^{i}Pr$_2$$C_6H_3$). ^{11}B NMR (128 MHz, benzene-d_6): δ −18.2. ^{15}N{^{1}H} NMR (71 MHz, benzene-d_6): δ −139.8 (CNCMe$_2$CH$_2$O), −236.6 (NH-2,6-^{i}Pr$_2$C$_6$H$_3$). IR (KBr, cm^{-1}): 3403 (vw), 3049 (w), 2962 (m), 2868 (m), 1621 (w), 1567 (s), 1461 (m), 1426 (s), 1384 (w), 1366 (w), 1329 (w), 1259 (s), 1191 (m), 1153 (m), 1109 (w), 1039 (w), 959 (m), 926 (w), 884 (w), 842 (m), 790 (w), 742 (m). Anal. Calcd. for $C_{45}H_{65}BN_5O_3Y$: C, 65.61; H, 7.95; N, 8.50. Found: C, 65.62; H, 8.22; N, 7.93. mp 155 °C (dec.).

Hydroamination Catalysis. In a typical experiment, an NMR tube equipped with a J. Young Teflon valve was charged with **1** (10 μmol), the appropriate substrate (0.2 mL of a 1 M solution in benzene-d_6; 200 μmol), and 0.3 mL of benzene-d_6. The ^{1}H NMR spectrum of the reaction mixture was recorded at regular intervals to accurately determine the time until complete conversion.

Kinetic Measurements. Reactions were monitored by ^{1}H NMR spectroscopy with a Bruker DRX400 spectrometer using 5 mm Wilmad NMR tubes equipped with a J. Young Teflon valve. Samples were prepared by dissolution of **1** in benzene-d_6 containing a known concentration of C_6Me_6 or C_8H_{16} standard and aminoolefin immediately before being placed in the NMR probe, which was preset to the required temperature. The probe temperature was calibrated before each measurement using an external thermocouple in an NMR tube lowered into the probe; once the probe temperature stabilized, it was monitored with the instrument's thermocouple. Single scan spectra were acquired automatically at preset time intervals. The peaks were integrated relative to C_6Me_6 or C_8H_{16} as an internal standard. Rate constants were obtained by nonweighted linear least-squares fit of the concentrations to the integrated rate law.

Results and Discussion

Synthesis and X-ray Structural Characterization of [Y(κ^3-To^M)(CH$_2$SiMe$_3$)$_2$(THF)] (1). Alkane elimination occurs upon treatment of [Y(CH$_2$SiMe$_3$)$_3$(THF)$_2$] with one equivalent of H[To^M] dissolved in minimal amounts of pentane and THF, respectively, at ambient temperature to afford the six-coordinate complex [Y(κ^3-To^M)(CH$_2$SiMe$_3$)$_2$(THF)] (**1**) in high isolated yield (77%, eq 3).

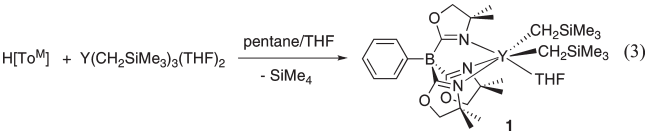

(3)

A single-crystal X-ray structure confirms the identity of **1** revealing κ^3-*N*,*N*,*N*-coordination of the To^M, one THF, and two trimethylsilylmethyl ligands bonded to yttrium (Figure 1). Although **1** is fluxional in solution as indicated by ^{1}H NMR spectroscopy (see below), only one specific and distorted geometry is observed in the solid state such that two independent molecules in the unit cell have similar metrical parameters. The tridentate To^M ligand is tied-back which results in small ∠N−Y1−N angles of 80.2(2), 79.9(2), and 75.7(2)°; the third angle is significantly smaller than the other two. The Y1−N bond distances of 2.443(5), 2.477(5), and 2.571(7) Å are also inequivalent, and the anomalously long bond is trans to one CH$_2$SiMe$_3$ rather than THF. The two shorter Y1−N bonds (2.477(5) and 2.443(5) Å) trans to the other CH$_2$SiMe$_3$ and to THF are statistically equivalent. Because the two Y1−N bond lengths trans to CH$_2$SiMe$_3$ are different by ca. 0.1 Å, it is surprising that the Y1−C distances 2.405(7) and 2.409(7) Å are identical. The angles between THF and the two CH$_2$SiMe$_3$ ligands are also very different: ∠O4−Y1−C26 is 83.5(3) and ∠O4−Y1−C22 is 99.7(2)°. Because both molecules in the unit cell have similar geometries, these distorted structural features are best explained by interligand steric interactions between the bulky To^M and CH$_2$SiMe$_3$ ligands and have little to do with electronic differences between CH$_2$SiMe$_3$ and THF ligands. The two CH$_2$SiMe$_3$ groups are oriented to avoid each other, forcing one CH$_2$SiMe$_3$ to be directed toward the THF ligand resulting in the large ∠O4−Y1−C22 angle. The other CH$_2$SiMe$_3$ points toward the CMe$_2$ group of an oxazoline ring, and that angle is also large (∠C26−Y1−N2 = 112.0(3)°).

Because yttrium(III) is relatively large (0.9 Å six-coordinate radius)[23] and distortions in the complex's

(23) Shannon, R. D. *Acta Crystallogr., Sect. A* **1976**, *32*, 751–767.

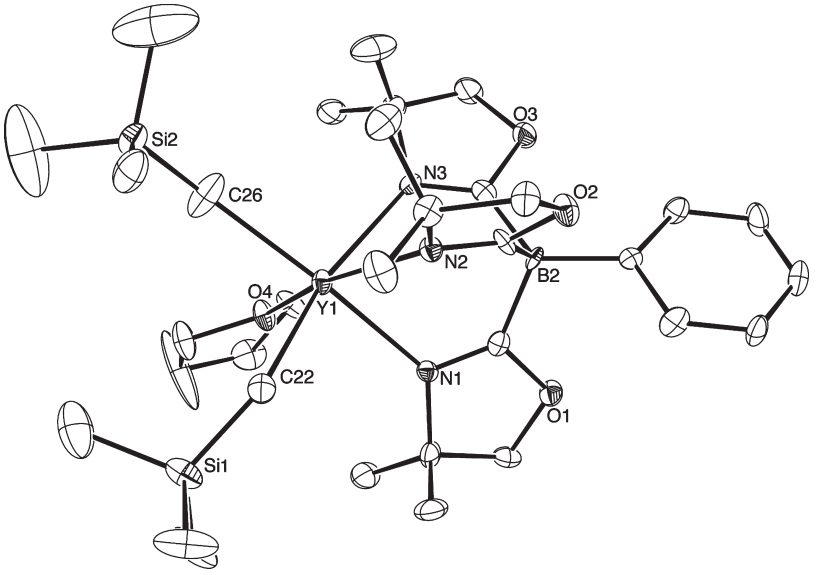

Figure 1. ORTEP diagram of one molecule of $[Y(\kappa^3\text{-}To^M)(CH_2SiMe_3)_2(THF)]$ (**1**) contained in the asymmetric unit at 50% probability. Hydrogen atoms and the second structurally related molecule are omitted for clarity.

geometry are due to interligand steric interactions, the effective steric properties of To^M bonded to yttrium were evaluated. The solid angle for a ligand, which is determined by treating the metal center as a point source of light and evaluating the surface area of the shadow cast by the ligand on a sphere surrounding the complex, provides a good method for evaluating the steric properties of ligands (particularly multidentate ligands).[24] In **1**, the solid angle of To^M (5.82 steradians) determined using the program Solid-G[25] corresponds to 46.3% of the surface area of the sphere. The solid angle of a CH_2SiMe_3 group is 1.74 steradians (13.9%) and THF is 1.6 steradians (13.0%). Because tridentate *N*,*N*,*N*-coordination is the only accessible bonding mode (see below), redistribution to give $[Y(\kappa^3\text{-}To^M)_2(CH_2SiMe_3)]$ and $[Y(CH_2SiMe_3)_3(THF)]$ is disfavored by the size of To^M even on the large yttrium center. Importantly, the solid angles and the X-ray structure also reveal that a hemisphere around the yttrium center (corresponding to three *fac*-sites of an octahedron) is available for reactivity.

For comparison, the X-ray structure of $[Y(\kappa^3\text{-}Tp^*)Cl_2(3,5\text{-}Me_2N_2C_3H)]$ reveals a similar tied-back geometry for the Tp* ligand (∠N−Y−N angles of 79.4(2), 79.3(2), and 78.6(2)°), Y−N bond distances of 2.368(6), 2.418(5), and 2.420(5) Å, and a slightly smaller solid angle for Tp* of 5.58 steradians (44.4% of the surface area of a sphere surrounding the complex is occupied).[10b]

Exchange Process in Compound 1. There is no crystallographic symmetry imposed upon **1** in the solid state ($Pna2_1$ space group), and the ligands' conformations give C_1-symmetric structures. However, the solid state and apparent solution symmetry are incongruent because of fluxional process(es), as only one set of oxazoline resonances (1.20 and 3.33 ppm, integrating to 18 and 6 H, respectively) are detected in the ^{1}H NMR spectrum of **1**, which is consistent with a C_{3v} symmetric To^M ligand (benzene-d_6 at room temperature). Both of these singlets correlate to a single oxazoline ^{15}N resonance at −141.7 ppm, as shown by a ^{1}H−^{15}N HMBC experiment; this indicates that the oxazolines are bonded to yttrium (cf. "free" 2*H*-4,4-dimethyl-2-oxazoline ^{15}N NMR: −127.5 ppm). Under these conditions, the two CH_2SiMe_3 groups are also equivalent and bonded to yttrium ($^2J_{YH}$ = 2.8 Hz, $^1J_{YC}$ = 35 Hz, $^2J_{YSi}$ = 4.6 Hz). THF is also coordinated (3.89 and 1.35 ppm, 4 H each), and only a single set of THF resonances is observed in the presence of excess THF in benzene-d_6 indicating that coordinated and free THF exchange rapidly at room temperature. Because the mechanism responsible for this observed symmetrization could involve oxazoline and/or THF dissociation, we investigated the fluxional process in detail to establish the labile or inert nature of the tris(oxazolinyl)borate ligand in **1**.

The low-temperature ^{1}H NMR spectrum of **1** (toluene-d_8, 220 K) contained three singlet resonances in a 1:1:1 ratio for oxazoline methyl groups as well as a pair of coupled doublets and a singlet for the methylene groups. Additionally, resonances corresponding to coordinated and free THF were observed (in the presence of excess THF). The low-temperature C_s-symmetric structure of **1** is depicted in Figure 2.[8a]

^{1}H NMR spectra of **1** were recorded between 200 and 280 K, and $[Y(\kappa^3\text{-}To^M)(CH_2SiMe_3)_2(THF)]$ is the only species detected over this temperature range. This indicates that temperature-dependent changes to the equilibria will not complicate our analysis of the exchange process. The resonances for free and coordinated THF decoalesce at 243 K, and resonances for C_s-symmetric To^M decoalesce at the same temperature, strongly suggesting that the fluxional process that exchanges the oxazoline groups is correlated with THF exchange. Additionally, the exchange process occurs in the absence of excess THF (to ^{1}H NMR detection limits). Therefore, we postulate that the mechanism for symmetrization of **1** involves a dynamic equilibri-

(24) (a) White, D.; Taverner, B. C.; Leach, P. G. L.; Coville, N. J. *J. Comput. Chem.* **1993**, *14*, 1042–1049. (b) White, D.; Coville, N. J. *Adv. Organomet. Chem.* **1994**, *36*, 95–158.

(25) (a) Guzei, I. A.; Wendt, M. *Dalton Trans.* **2006**, 3991–3999. (b) Guzei, I. A.; Wendt, M. *Program Solid-G*; University of Wisconsin: Madison, WI, 2004.

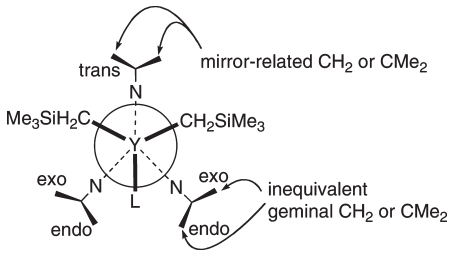

Figure 2. Newman projection of **1** (L = THF) or **2** (L = $OPPh_3$) looking along the Y−B axis. The groups attached to N represent CH_2 or CMe_2 of an oxazoline ring.

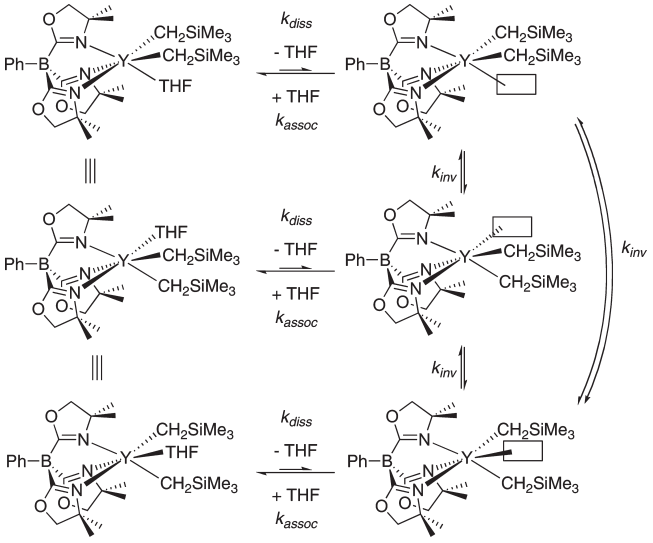

Figure 3. Proposed mechanism for symmetrization of [Y(κ^3-To^M)-(CH_2SiMe_3)$_2$(THF)] (**1**). The process involves a THF dissociation/coordination at equilibrium, with $k_{diss} \ll k_{assoc}$, followed by rapid inversion of the five-coordinate yttrium(III) species. The open coordination sites on the five-coordinate species are illustrated to clarify the overall site exchange and do not imply a particular geometry (square pyramidal or trigonal bipyramidal) or mechanism (turnstile or pseudorotation) for site exchange.

um that favors **1** and proceeds via THF dissociation, inversion of a five-coordinate yttrium species, followed by THF coordination (Figure 3).

The dynamic behavior of both the methyl and methylene regions was simulated using gNMR,[26] and this simulation provides rate constants for site exchange of three oxazoline groups. The rate constants, measured at concentrations of [**1**] = 35.7 and 71.4 mmol (e.g., $k_{exchange}^{225K} = 7\ s^{-1}$), are independent of [**1**] and unaffected by added equivalents of THF. An Eyring plot, using the rate constants obtained from dynamic NMR simulations, provides values of $\Delta H^{\ddagger} = 80.1 \pm 1.5$ kJ mol^{-1} (19.1 ± 0.4 kcal mol^{-1}) and $\Delta S^{\ddagger} = 124 \pm 6$ J mol^{-1} K^{-1} (30 ± 1 eu). These activation parameters are clearly consistent with a dissociative exchange process because the large $\Delta H^{\ddagger}$ is consistent with bond breaking and the large positive $\Delta S^{\ddagger}$ indicates increased disorder in the transition state. These parameters indicate that the rate determining step in the overall exchange process is THF dissociation rather than coordination (where the opposite sign for $\Delta S^{\ddagger}$ is expected); this dissociation is also consistent with the observed [THF]-independent exchange rates and the observation of **1** as the only To^{M}Y-containing species present. Yttrium inversion and oxazoline-arm dissociation are also unlikely since $\Delta S^{\ddagger}$ is large, and this mechanism suggests that k_{inv} is fast with respect to THF dissociation. The entropic and enthalpic contributions to the activation barrier are counterbalanced and give a small overall $\Delta G^{\ddagger}$ (50.0 kJ mol^{-1} or 11.9 kcal mol^{-1}) at the coalescence temperature of 243 K.

For comparison, the compound [Y(κ^3-Tp*)Cl_2(THF)] is fluxional to at least 200 K in THF-d_8, but in 3,5-dimethyltetrahydrofuran a static C_s-symmetric structure for [Y(κ^3-Tp*)Cl_2(3,5-$Me_2OC_4H_6$)] is observed (i.e., slow exchange occurs with a bulkier ligand) suggesting that the ligand exchange mechanism in this pyrazolylborate system is associative.[10b] Additional evidence for associative substitution in the Tp-system is that the parent [Y(κ^3-Tp)-X_2(THF)$_2$] (X = Cl, Br) compounds are seven-coordinate.[10b] The different spatial distribution of steric bulk in To^M versus Tp* may be responsible for this mechanistic change, although the difference in chloride versus alkyl ligand may also affect the mechanism. [Y(κ^3-Tp*)(CH_2SiMe_3)$_2$(THF)] is fluxional at room temperature, but no mechanism is proposed for exchange.[10,11] While 3,5-dimethyl pyrazole in Tp* is planar and provides a sterically open coordination site for a second THF to bind, oxazoline groups are nonplanar and their 4,4-dimethyl groups are directed toward the THF ligand's coordination site (See Figure 2 above), and this may facilitate THF dissociation.

Reactions of Compound 1: Substitutions and Bis(Amido) Syntheses. Although **1** is unchanged after weeks at room temperature in the solid state, its benzene-d_6 solutions produce Me_4Si and THF as the ^{1}H NMR resonances corresponding to **1** disappear over one day at room temperature. New resonances corresponding to yttrium-To^M containing products are broad and the species formed have not been identified; however the To^M ligand itself has not decomposed since exposure of this solution to air gives H[To^M]. The extrusion of $SiMe_4$ from **1** in solution is inhibited by excess THF, and after rapid displacement of the labile THF by THF-d_8, spectra of **1** are unchanged over two days in THF-d_8 at room temperature. These observations suggest that the pathway for decomposition of **1** involves THF dissociation as a first step. Because To^M is ancillary in the symmetrization and decomposition processes, substitution reactions of the THF and alkyl ligands were investigated.

Addition of $OPPh_3$ to a benzene-d_6 solution of **1** produces THF and [Y(κ^3-To^M)(CH_2SiMe_3)$_2$($OPPh_3$)] (**2**); the formation of **2** was easily verified by a $^{31}P\{^1H\}$ NMR spectrum that contained a doublet resonance at 36.69 ppm coupled to yttrium (d, $^2J_{YP} = 9.8$ Hz). The phosphine oxide ligand in **2** is labile, but its exchange is slower than THF exchange in **1**. Thus at room temperature in toluene-d_8, broad oxazoline resonances in the ^{1}H NMR spectrum of **2** were consistent with a C_s-symmetric structure slowly exchanging on the NMR time scale (see Figure 2, L = $OPPh_3$). Due to this exchange process, crosspeaks were not observed in a $^1H-^{15}N$ HMBC spectrum, thus nitrogen chemical shifts could not be determined for **2**.[27] At 270 K, sharp peaks in

(26) Budzelaar, P. H. M. *gNMR*, v. 5.0; IvorySoft.

(27) Variable-temperature NMR spectra could not be acquired with a Bruker *Z*-gradient inverse TXI $^1H/^{13}C/^{15}N$ 5 mm cryoprobe.

the ^{1}H NMR spectrum of the static C_s-symmetric structure were observed. The coalescence temperature for oxazoline exchange is 320 K, as compared to 243 K for **1**, and this T_C is unaffected by added $OPPh_3$. An Eyring plot based on line shape analysis provides the following activation parameters: $\Delta H^{\ddagger} = 71 \pm 1.1$ kJ mol^{-1} (17 ± 0.3 kcal mol^{-1}) and $\Delta S^{\ddagger} = 26 \pm 1$ J mol^{-1} K^{-1} (6.2 ± 0.2 e.u.). The positive $\Delta S^{\ddagger}$ and zero-order dependence on [$OPPh_3$] are again consistent with a dissociative mechanism. However, we were surprised to find similar $\Delta H^{\ddagger}$ but a significantly smaller $\Delta S^{\ddagger}$ value for **2** versus **1**.

One possible explanation for the low activation entropy in **2** is that oxazoline-arm dissociation, which is expected to have a small dependence on entropy, is occurring rather than $OPPh_3$ dissociation. However, several other experiments rule out this interpretation. In the presence of 3 equiv. of $OPPh_3$, **2** is the only To^M-containing species observed, and there is no evidence for a bis(phosphine oxide) species that might be formed upon oxazoline dissociation. Phosphine oxide exchange is occurring, and support for this comes from the reaction of $OPPh_2Cy$ and **2**, which gives a mixture containing **2**, free $OPPh_3$, [Y(κ^3-To^M)(CH_2SiMe_3)$_2$($OPPh_2Cy$)], and $OPPh_2Cy$ (assigned by ^{31}P NMR spectroscopy) after 10 min at room temperature in benzene-d_6. Variable-temperature ^{31}P NMR spectra of a mixture of **2** and $OPPh_3$, acquired from 270 to 360 K in toluene-d_8, show resonances for **2** and free $OPPh_3$ that broaden as the temperature increases. Broad resonances in the high-temperature spectra prove that free and coordinated phosphine oxide exchange rapidly on the ^{31}P NMR time scale. If oxazoline-arm dissociation rather than $OPPh_3$ dissociation was involved in the symmetrization process (observed in the ^{1}H NMR spectra), then the resonance due to free $OPPh_3$ would not be broadened. These ^{31}P NMR spectra were simulated with gNMR[26] to obtain rate constants for exchange of free and coordinated phosphine oxide. From these data, activation parameters for exchange of coordinated phosphine oxide in **2** with free phosphine oxide ($\Delta H^{\ddagger} = 80 \pm 4$ kJ mol^{-1}; $\Delta S^{\ddagger} = 23 \pm 1$ kJ mol^{-1}K^{-1}) are comparable to the parameters determined from the ^{1}H NMR spectra for the symmetrization process in **2**, and this suggests that both processes have a common mechanism. Taken together, these observations strongly favor $OPPh_3$ dissociation as the rate determining step for the symmetrization of **2** observed at elevated temperatures.

We propose that the low activation entropies measured for symmetrization and exchange processes in **2** result from an early transition state for $OPPh_3$ dissociation where bond cleavage is less compensated by entropic factors (in comparison to THF dissociation from **1**). As expected from qualitative analysis of variable-temperature NMR spectra, the $\Delta G^{\ddagger}$ value at the coalescence temperature (62.7 kJ mol^{-1}; 15.0 kcal mol^{-1} at 320 K) for $OPPh_3$ dissociation is significantly higher than the value measured for THF dissociation (50.0 kJ mol^{-1}; 11.9 kcal mol^{-1} at 240 K). Significantly, these measurements set a lower limit for the Gibbs Free Energy barrier for oxazoline-arm dissociation to be >15 kcal mol^{-1} (at least for compound **2** at 320 K), and this limit likely applies to other tris(oxazolinyl)borate yttrium compounds as well.

Reactions of **1** and two equivalents of the small primary amines ^{t}BuNH$_2$ and *para*-$MeC_6H_4NH_2$ afford six-coordinate bis(amido)yttrium compounds [Y(κ^3-To^M)(NH^{t}Bu)$_2$(THF)] (**3**) and [Y(κ^3-To^M)(NH-*para*-Me-C_6H_4)$_2$(THF)] (**4**) along with two equivalents of Me_4Si within 5 min at room temperature, as determined by ^{1}H NMR spectroscopy (eq 4). As in bis(alkyl) **1**, bis(amido) THF adducts **3** and **4** are fluxional, so the To^M ligand appears C_{3v} symmetric in their ^{1}H NMR spectra.

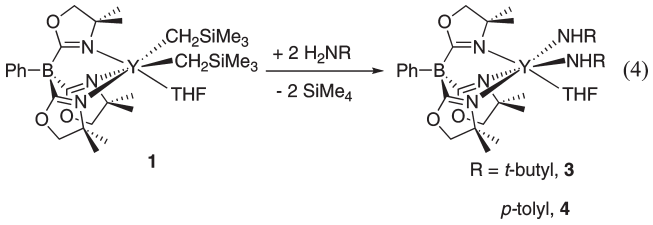

(4)

Addition of 3 equiv. of ^{t}BuNH$_2$ to **1** produces a mixture of THF adduct **3** and amine adduct [Y(κ^3-To^M)(NH^{t}Bu)$_2$(^{t}BuNH$_2$)] (**5**). These two species undergo rapid exchange on the ^{1}H NMR time scale, and only one set of To^M resonances is observed (see below). Pure samples of compound **5** are isolated by addition of excess ^{t}BuNH$_2$ to a benzene solution of **1** (or the mixture of **3** and **5**) followed by evaporation of the volatile materials. Bis(amido)amine **5** crystallizes from a concentrated toluene solution layered with pentane at -30 °C. A low-resolution X-ray structure verifies its identity as a six-coordinate yttrium center bonded to three oxazoline nitrogens and three N^{t}Bu-containing ligands (see the Supporting Information). The ^{1}H NMR spectrum of **5** (benzene-d_6, room temperature) contains one set of sharp To^M resonances (the oxazolines are equivalent), one broad *tert*-butyl resonance (27 H), and a broad NH resonance (4 H). As in compounds **1**−**4**, fluxional exchange processes result in the symmetrization of the To^M ligand which appears C_{3v} symmetric. However, in **5**, the symmetrization process(es) could involve amine ligand dissociation/coordination and/or proton transfer between amine and amido ligands (see Figure 4).

Therefore, low-temperature ^{1}H NMR spectra of **5** are very interesting. When a solution of **5** in toluene-d_8 is cooled to 250 K, the oxazoline resonances remain sharp. However, the broad ^{t}Bu peak reaches its coalescence temperature at 260 K. At 240 K, two distinct *tert*-butyl resonances appear in a 2:1 ratio that correspond to the two *tert*-butylamides and one coordinated *tert*-butylamine, respectively. The amide peak is relatively sharp, whereas the amine resonance is broad, and the decoalescence of these two signals corresponds to slowing of intramolecular proton transfer from the amine to an amido ligand. Desymmetrization of the oxazoline groups begins to occur below 250 K, with a T_C of 220 K. At 190 K, the spectrum is broad but its straightforward interpretation is consistent with a C_s-symmetric structure for [Y(κ^3-To^M)(NH^{t}Bu)$_2$(^{t}BuNH$_2$)], where amine dissociation/coordination and proton exchange are slow on the ^{1}H NMR time scale. Importantly, signals corresponding to both free and bound *tert*-butylamine could be observed at this temperature in the presence of excess ^{t}BuNH$_2$. These data support symmetrization mechanisms

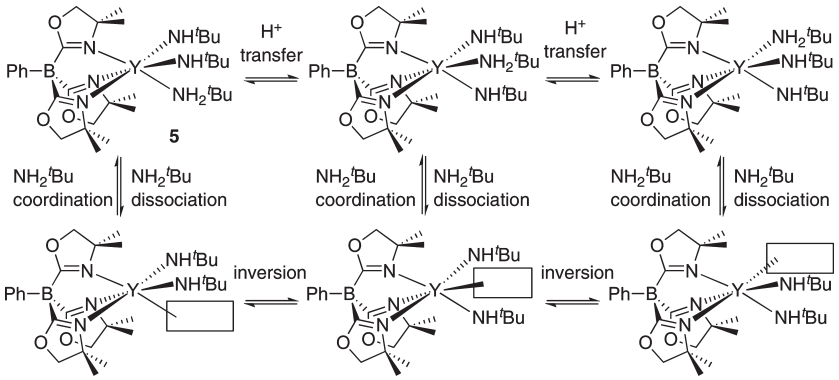

Figure 4. Exchange processes occurring in [Y(κ^3-To^M)(NH^{t}Bu)$_2$(^{t}BuNH$_2$)] (**5**). Variable-temperature ^{1}H NMR spectroscopic data indicate that proton transfer is slow relative to amine dissociation.

for **5** that involve *both* amine dissociation/coordination and proton exchange between coordinated amine and amide ligands (see Figure 4). In fact, we conclude that intramolecular proton transfer from a coordinated amine to an amido ligand is slower than amine dissociation/coordination (for this system). Unfortunately, a detailed kinetic study of this system is precluded by the relatively similar rates for the two processes; qualitative comparisons of the spectra indicate that amine dissociation in **5** is faster than THF dissociation in bis(alkyl) **1**. In the bent lanthanocene Cp*$_2$LaNHR(NRH$_2$) (R = Me, Et), intramolecular proton transfer is slow at 173 K.[13b] In that case, the observed low-temperature structure is C_s-symmetric due to either a mirror plane in the static structure or a second exchange process that is fast on the NMR time scale at 173 K.[13b]

Additionally, we compared the relative binding affinity of THF versus ^{t}BuNH$_2$ as neutral ligands (L) for the metal center in [Y(κ^3-To^M)(NH^{t}Bu)$_2$(L)]. Addition of three equivalents of ^{t}BuNH$_2$ to **1** in benzene-d_6 produces a single set of oxazoline resonances in the ^{1}H NMR spectrum at room temperature, and neither free THF nor free ^{t}BuNH$_2$ are observed because of their involvement in rapid dissociation/coordination processes. The spectra are broad even at 190 K in toluene-d_8, although oxazoline resonances consistent with C_s-symmetric structures of **3** and **5** are observed at that temperature, as well as two resonances due to *tert*-butylamide ligands in **3** and **5**. Resonances for free and bound THF are also evident, as well as free ^{t}BuNH$_2$. Apparently, **3** and **5** have similar formation constants and in the presence of equal quantities of THF and ^{t}BuNH$_2$ both are present. Integration of free ^{t}BuNH$_2$ and THF resonances (or the *tert*-butylamide groups of **3** and **5**) in the ^{1}H NMR spectrum recorded at 190 K indicates that **3** and **5** are present in a 1.2:1 ratio. Thus, THF is a slightly better ligand for the putative five-coordinate [Y(κ^3-To^M)(NH^{t}Bu)$_2$] than ^{t}BuNH$_2$.

Good support for the intermediacy of five-coordinate yttrium(III) centers in the To^{M}Y-system is provided by sterically hindered amines. In particular, the larger primary aniline 2,6-^{i}Pr$_2$C$_6$H$_3$NH$_2$ reacts to form the THF-free five-coordinate species [Y(κ^3-To^M)(NH-2,6-^{i}Pr$_2$C$_6$H$_3$)$_2$] (**6**, eq 5). The To^M ligand appears C_{3v}-symmetric in **6**, which is incommensurate with a static five-coordinate species, and thus this compound is also fluxional. The ^{15}N NMR resonance for the oxazolinyl groups in To^M (−139.8 ppm), observed with a ^{1}H−^{15}N HMBC experiment, are far downfield of the yttrium amide resonance (−236.6 ppm, detected by a one-bond ^{1}H−^{15}N HMQC experiment). Unlike six-coordinate compounds **1**−**5**, the apparent symmetry of the To^M ligand in five-coordinate **6** is C_{3v} even to 190 K. Thus, inversion of the 5-coordinate yttrium center in **6** (presumably via a pseudo-rotation or turnstile mechanism) is faster than the NMR time scale. Importantly, this observation rules out yttrium inversion as the rate determining step in the symmetrization process for **1** and provides additional support for THF dissociation as the slowest step.

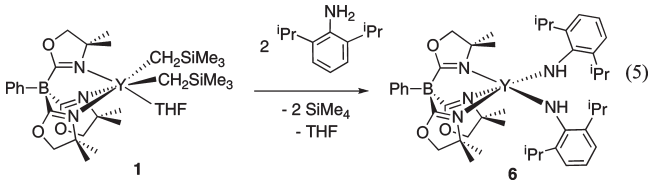

Catalytic Hydroamination. The catalytic competence of tris(oxazolinyl)borate-containing rare earth compounds was established using hydroamination/cyclization of aminopentenes as a test reaction. Since tris(pyrazolyl)-borate and tris-ox rare earth compounds have not been reported to catalyze hydroamination reactions, this study demonstrates new catalytic chemistry for compounds containing monoanionic *fac*-coordinating ligands. The substituted substrates 2,2-diphenyl-4-penten-1-amine (**7**) and 2,2-dimethyl-4-penten-1-amine (**8**) are cyclized by 5 mol % **1** in benzene-d_6 to form the corresponding 2-methylpyrrolidine products in quantitative yield. Cyclizations of diphenyl-substituted **7** proceed readily at room temperature, whereas reactions of **8** require 50 °C for efficient conversion. In addition, the OPPh$_3$ adduct **2** and the five-coordinate bis(anilido) complex **6** were also tested as precatalysts for the cyclization of diphenyl substrate **7**. Compared to **1**, conversion is only slightly faster with 5-coordinate precatalyst **6**, and much slower in the presence of the strongly coordinating OPPh$_3$ ligand in **2**. Additionally, the secondary amine substrate **9** is also readily cyclized by **1** to form the *N*-methylpyrrolidine product, but the tris(oxazolinyl)borate yttrium catalysts are unable to cyclize the unsubstituted 4-penten-1-amine (**10**). The results of these studies are summarized in Table 1.

Table 1. Hydroamination Cyclization Catalyzed by Tris(oxazolinyl)boratoytrium(III) Complexes; Typical Conditions: Benzene-d_6, 400 mM [substrate], 20−25 mM [catalyst]

Entry	Substrate	Product	Precatalyst	T (°C)	N_t (h^{-1})[a]
1.	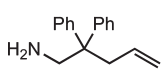 **7**	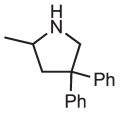	**1**	22	2.4
2.	**7**		**1**	37	8.2
3.	**7**		**2**	37	3.2
4.	**7**		**6**	37	9.0
5.	 **8**	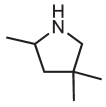	**1**	50	1.9
6.	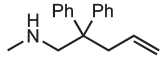 **9**	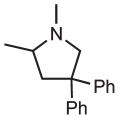	**1**	37	2.2[b]
7.	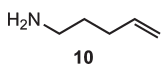 **10**		**1**	100	trace product

[a] N_t = rate/[catalyst]. Rate was calculated from the slope of linear plots of [substrate]/time through three half-lives. [b] Clean zero-order kinetics were not observed for 3 half-lives; N_t calculated from conversion of substrate through two half-lives.

The catalytic activity of complexes **1**, **2**, and **6** for the hydroamination/cyclization of substrates **7** and **8** is rather modest with respect to highly active lanthanocene catalysts. For example, cyclization of the *gem*-dimethyl substrate **8** with catalyst **1** proceeded with a turnover frequency of 1.9 h^{-1} at 50 °C, compared to 95 h^{-1} at 25 °C for [Cp*$_2$LaCH(SiMe$_3$)$_2$].[13b] Marks has reported that lanthanide bis(oxazoline) catalysts are extremely efficient in asymmetric hydroamination/cyclization reactions; a catalyst system derived from (4*R*,5*S*)-Ph$_2$BoxH (Box = 2,2′-bis(2-oxazoline)methylenyl) and [La{N(SiMe$_3$)$_2$}$_3$] cyclizes *gem*-diphenyl substrate **7** at 23 °C with a turnover rate exceeding that of catalyst **1** by several orders of magnitude (660 h^{-1} vs 2.4 h^{-1}).[20] The activity of catalyst **1** for aminoalkene **8** is more comparable to other nonmetallocene yttrium-based hydroamination catalysts. The simple homoleptic tris(amide) complex [Y{N(SiMe$_3$)$_2$}$_3$] cyclizes **8** with a turnover frequency of 11.6 h^{-1} at 25 °C,[28] and well-defined yttrium alkyl and amido complexes supported by diamidoamine ligands catalyze the same reaction with turnover rates between 1.2 and 10 h^{-1}.[28b]

Kinetics of the cyclization of 2,2-diphenyl-4-penten-1-amine substrate (0.4 M) catalyzed by **1** (4−10 mol %) were evaluated at 310 K; the rate is independent of [substrate] for 3 half-lives (see the Supporting Information). Zero-order substrate dependence is not a result of saturation kinetics, since high catalyst loadings also provide linear plots of [substrate] versus time for three half-lives. Additionally, curves obtained by plotting product concentration versus time also are linear over the observed reaction time. A plot of reaction rate versus precatalyst concentration for a constant [substrate]$_0$ is linear over the measured concentration range (17.1−40.8 mM), indicating a first-order dependence on [**1**]. The resulting rate law, $-d$[substrate]$/dt = k_{obs}$[**1**]^1[substrate]^0, is consistent with the commonly postulated mechanism for rare earth element-catalyzed intramolecular hydroamination reactions in which the turnover limiting step is an alkene insertion.[13] A nonzero (negative) intercept and slope $\neq 1$ for a plot of k_{obs} versus [catalyst] indicates that a portion of the catalytic sites are deactivated during the reaction, presumably by reversible binding of a ligand to the sixth coordination site on yttrium(III) inhibiting conversion. The primary amine substrate, secondary amine product, and THF are all likely inhibitors. In fact, the formation of [Y(κ^3-To^M)-(NH^{t}Bu)$_2$(^{t}BuNH$_2$)] (**5**) in the presence of excess ^{t}BuNH$_2$ suggests that the resting state of the catalyst during hydroamination catalysis is an amine adduct since excess amine is present under catalytic conditions. The X-ray diffraction study of **5** provides a model for the structure of the catalyst's resting state (see above). Interestingly, increasing [**1**] increases the observed rate (and presumably the percentage of active sites) in a linear but greater-than-unity fashion. As the concentration of **1** is increased at higher loadings, [yttrium] and [THF] increase in a strictly 1:1 fashion, whereas the yttrium:amine ratio changes as catalyst concentration is increased. Since greater inhibition is observed at low catalyst loadings, we suggest that amine coordination is more significant to catalyst inhibition than THF binding. Because the rate is essentially invariant over the reaction time, product and substrate coordination to yttrium contribute approximately equally to the inhibition.[13b,18h] Similar catalytic activities are observed for **1** and the THF-free precatalyst **6** in the cyclization of diphenyl substrate **7** (Table 1, entries 2 and 4) which is consistent with the proposal that amine coordination is more significant than THF binding in catalysis inhibition. However, the coordination of OPPh$_3$ to the active catalyst formed from **2** apparently becomes competitive with amine coordination and the turnover frequency is decreased by a factor of 3 (entry 3).

Conclusion

We have shown here that the tridentate monoanionic tris(oxazolinyl)borate To^M ligand supports six-coordinate bis(alkyl) and five- and six-coordinate bis(amido) yttrium complexes. The bowl-like To^M ligand occupies almost a hemisphere of space around the yttrium center as quantified by solid angles, and this disfavors disproportionation to mixtures of YR$_3$ and bis(To^M)YR-type complexes. However, the bulky To^M ligand does not impede substitution reactions in [Y(κ^3-To^M)(CH$_2$SiMe$_3$)$_2$(THF)] since THF is labile and easily replaced by OPPh$_3$ and amines. Furthermore, THF substitution occurs dissociatively through a five-coordinate intermediate, and this is contrasted with associative THF

(28) (a) Kim, Y. K.; Livinghouse, T.; Bercaw, J. E. *Tetrahedron Lett.* **2001**, *42*, 2933–2935. (b) Hultzsch, K. C.; Hampel, F.; Wagner, T. *Organometallics* **2004**, *23*, 2601–2612.

substitution in $[Y(\kappa^3\text{-Tp*})Cl_2(THF)]$[10] as well as the isolated seven-coordinate Tp^*YX_2(bipyridine) compounds.[14] The alkyl ligands in **1** react rapidly with amines to form bis(amides), and this reaction occurs even for relatively hindered amines such as 2,6-diisopropylaniline. We have also found that the amido ligands in complex **5** rapidly exchange with the amine ligands, and the coordinated amine is rapidly substituted by free amine. Qualitative inspection of variable temperature ^{1}H NMR spectra indicates that ^{t}BuNH$_2$ dissociation from **5** is faster than THF dissociation from **1**. Intramolecular proton transfer between amine and amido ligands is slower than both dissociative processes in these systems. Intramolecular proton transfer may be slow since some geometric distortion is necessary for the proton to bridge between two nitrogen ligands (N···N distance = 3.3−3.5 Å).

The robust To^M−Y interactions and labile Y−L coordination are important for the catalytic activity of these complexes. We have found that **1** is an active precatalyst for hydroamination/cyclization of aminoolefins even though much of the yttrium is tied up in dormant six-coordinate states such as $[Y(\kappa^3\text{-To}^M)(NHR)_2(THF)]$ or $[Y(\kappa^3\text{-To}^M)(NHR)_2(NH_2R)]$ ($R = CH_2CR'_2CH_2CH{=}CH_2$). However, the isolation and characterization of $[Y(\kappa^3\text{-To}^M)(NH\text{-}2,6\text{-}^i Pr_2C_6H_3)_2]$ indicates that sufficient steric pressure favors five-coordinate species in this class of compounds. Thus, we are currently preparing more hindered oxazolinylborate ligands to destabilize six-coordinate geometries and enhance catalytic activity in hydroamination, as well as synthesizing optically active tris(oxazolinyl)borate rare earth compounds for stereoselective catalytic hydroamination reactions.

Acknowledgment. Support was provided by the Roy J. Carver Charitable Trust and the ACS Green Chemistry Institute-Petroleum Research Fund. We thank Bruce Fulton for assistance with ^{1}H−^{15}N HMBC experiments.

Supporting Information Available: Variable-temperature ^{1}H and ^{31}P NMR spectra for **1** and **2**, Eyring plots from line shape analysis, plots of conversion versus time for hydroamination catalysis, and X-ray crystallographic data for **1** and **5** (PDF). This material is available free of charge via the Internet at http://pubs.acs.org.